Quantum Monte Carlo Simulations of the Half-Filled Two-Dimensional Kondo Lattice Model

F. F. Assaad

Institut für Theoretische Physik III, Universität Stuttgart, Pfaffenwaldring 57, D-70550 Stuttgart, Germany

(Received 13 April 1999)

The 2D half-filled Kondo lattice model with exchange J and nearest neighbor hopping t is considered. It is shown that this model belongs to a class of Hamiltonians for which zero-temperature auxiliary field Monte Carlo methods may be efficiently applied. We compute the staggered moment and spin and quasiparticle gaps on lattice sizes up to 12×12. The competition between the RKKY interaction and Kondo effect leads to a continuous quantum phase transition between antiferromagnetic and spin-gapped insulators. This transition occurs at $J/t = 1.45 \pm 0.05$.

PACS numbers: 71.27.+a, 71.10.Fd

The Kondo lattice model (KLM) describes a band of conduction electrons interacting with local moments via an exchange interaction J. This model is relevant for the understanding of heavy electron materials [1,2]. The nature of the ground state results from competing effects. The polarization cloud of conduction electrons produced by a local moment may be felt by another local moment. This provides the mechanism for the Ruderman-Kittel-Kasuya-Yosida (RKKY) interaction [3] with effective exchange $J_{\mathrm{eff}}(\vec{q}) \propto -J^2\,\mathrm{Re}\chi(\vec{q}, \omega = 0)$, $\chi(\vec{q}, \omega)$ being the spin susceptibility of the conduction electrons. On the other hand, the same polarization cloud may form a singlet bound state with the local moment. In the single impurity case, this happens at the Kondo temperature $T_K \propto \epsilon_f e^{-1/JN(\epsilon_f)}$, where ϵ_f is the Fermi energy and $N(\epsilon_f)$ is the density of states [4]. Comparing energy scales, the RKKY interaction dominates at *small* J and the Kondo effect dominates at *large* J. Thus a quantum transition between magnetically ordered and disordered phases is anticipated.

The KLM we consider is written as

$$H_{\mathrm{KLM}} = -t \sum_{\langle \vec{i},\vec{j}\rangle,\sigma} c^{\dagger}_{\vec{i},\sigma} c_{\vec{j},\sigma} + J \sum_{\vec{i}} \vec{S}^{c}_{\vec{i}} \vec{S}^{f}_{\vec{i}} \,. \qquad (1)$$

Here $\vec{i}$ runs over the L^2 sites of a square lattice, $\langle \vec{i}, \vec{j} \rangle$ corresponds to nearest neighbors, $c^{\dagger}_{\vec{i},\sigma}$ ($f^{\dagger}_{\vec{i},\sigma}$) creates a conduction (localized) electron with a z component of spin σ on site $\vec{i}$, and periodic boundary conditions are imposed. $\vec{S}^{f}_{\vec{i}} = (1/2) \sum_{\sigma,\sigma'} f^{\dagger}_{\vec{i},\sigma} \vec{\sigma}_{\sigma,\sigma'} f_{\vec{i},\sigma'}$ and $\vec{S}^{c}_{\vec{i}} = (1/2) \sum_{\sigma,\sigma'} c^{\dagger}_{\vec{i},\sigma} \vec{\sigma}_{\sigma,\sigma'} c_{\vec{i},\sigma'}$ with $\vec{\sigma}$ being the Pauli matrices. A constraint of one fermion per f site is enforced. At $J/t \ll 1$ this model maps onto the periodic Anderson model (PAM) [5] at strong coupling [6]. Quantum Monte Carlo (QMC) [7] methods constitute an efficient tool for the study of the PAM in various dimensions [8–10]. The one-dimensional version of the KLM has been extensively studied [11]. In particular, at $\langle n \rangle = 2$ (half-band filling or one conduction electron per local moment), the Kondo effect dominates at all values of J/t. In two dimensions, variational Monte Carlo methods [12] as well as series expansions around the strong coupling limit [13] support the existence of a critical point. The aim of this paper is to go beyond the above approximative approaches. We show how to efficiently simulate the KLM with the projector QMC (PQMC) algorithm [14,15]. This method yields *exact* zero-temperature results and is free of the notorious sign problem at half-band filling. This stands in contrast to previous approaches [16] which generate a sign problem even at $\langle n \rangle = 2$. Using this algorithm, we study the half-filled case as a function of J/t.

Our starting point is the Hamiltonian,

$$H = -t \sum_{\langle \vec{i},\vec{j}\rangle,\sigma} c^{\dagger}_{\vec{i},\sigma} c_{\vec{j},\sigma} - \frac{J}{4} \sum_{\vec{i}} \left[\sum_{\sigma} c^{\dagger}_{\vec{i},\sigma} f_{\vec{i},\sigma} + f^{\dagger}_{\vec{i},\sigma} c_{\vec{i},\sigma} \right]^2 + U_f \sum_{i} (n^{f}_{\vec{i},\uparrow} - 1/2)(n^{f}_{\vec{i},\downarrow} - 1/2) \,. \qquad (2)$$

with $n^{f}_{\vec{i},\sigma} = f^{\dagger}_{\vec{i},\sigma} f_{\vec{i},\sigma}$. This Hamiltonian has all the properties required for an efficient use of QMC methods. To avoid working with continuous fields, we use the approximate Hubbard-Stratonovitch (HS) transformation introduced in Refs. [17,18] to decouple the J term. This transformation introduces systematic errors of the order $(\Delta\tau)^3$, where $\Delta\tau$ corresponds to an imaginary time step. Since this order is higher than the systematic error produced by the Trotter decomposition, it is negligible. As for the Hubbard term, we have found it essential to use Hirsch decomposition in terms of Ising spins which couple to the density rather than to the z component of the magnetization [19]. Although this forces us to work with complex numbers, it conserves SU(2) symmetry for a given HS configuration. As argued in Ref. [20], this provides an efficient algorithm for the calculation of imaginary time displaced spin-spin correlation functions [21] from which we will determine the spin gap. The ground state of H (2), $|\Psi_0\rangle$, is obtained by projection. A trial wave function, $|\psi_T\rangle$, required to be a single Slater determinant and nonorthogonal to the ground state is propagated along the imaginary time axis till convergence is reached [14,15]. With the above HS transformations and the appropriate choice of $|\Psi_T\rangle$ [17], particle-hole symmetry leads to the absence of the sign problem at $\langle n \rangle = 2$.

The relation of the above model to the KLM model is seen by rewriting Eq. (2) as

 0031-9007/99/83(4)/796(4)$15.00

$$H = -t \sum_{\langle \vec{i},\vec{j}\rangle,\sigma} c^{\dagger}_{\vec{i},\sigma} c_{\vec{j},\sigma} + J \sum_{\vec{i}} \vec{S}^{c}_{\vec{i}} \vec{S}^{f}_{\vec{i}} - J \sum_{\vec{i}} (c^{\dagger}_{\vec{i},\sigma} c^{\dagger}_{\vec{i},-\sigma} f_{\vec{i},-\sigma} f_{\vec{i},\sigma} + \text{H. c.}) + J \sum_{\vec{i}} (n^{c}_{\vec{i}} n^{f}_{\vec{i}} - n^{c}_{\vec{i}} - n^{f}_{\vec{i}}) + U_f \sum_{i} (n^{f}_{\vec{i},\uparrow} - 1/2)(n^{f}_{\vec{i},\downarrow} - 1/2) . \quad (3)$$

with $n^{f}_{\vec{i}} = \sum_{\sigma} f^{\dagger}_{\vec{i},\sigma} f_{\vec{i},\sigma}$ and $n^{c}_{\vec{i}} = \sum_{\sigma} c^{\dagger}_{\vec{i},\sigma} c_{\vec{i},\sigma}$. It is important to notice that

$$\left[H, \sum_{\vec{i}} (1 - n^{f}_{\vec{i},\uparrow})(1 - n^{f}_{\vec{i},\downarrow}) + n^{f}_{\vec{i},\uparrow} n^{f}_{\vec{i},\downarrow} \right] = 0 . \quad (4)$$

The number of doubly occupied and empty f sites is a conserved quantity. Denoting by P_n the projection onto the subspace with n doubly occupied and empty f sites, one obtains

$$HP_0 = H_{\mathrm{KLM}} - N(U_f/4 + J) . \quad (5)$$

Thus, in principle, it suffices to consider a trial wave function satisfying $P_0|\Psi_T\rangle = |\Psi_T\rangle$ to ensure that $\exp(-\Theta H)|\Psi_T\rangle = \exp(-\Theta H_{\mathrm{KLM}})|\Psi_T\rangle$. The coupled constraints: $P_0|\Psi_T\rangle = |\Psi_T\rangle$, and $|\Psi_T\rangle$ is a Slater determinant forces us to choose $S^{f,z}_{\vec{i}}|\Psi_T\rangle = \pm\frac{1}{2}|\Psi_T\rangle$, thus breaking SU(2) spin symmetry. Since the KLM conserves total spin, this symmetry has to be restored by the imaginary time propagation. When the energy gap to the first excited spin state is small—as is certainly the case when long-range magnetic order is present—restoring this symmetry is extremely expensive. To avoid this problem and since the ground state of the KLM at half-filling on a bipartite lattice has $S = 0$ [22,23], we choose a spin singlet trial wave function. During the imaginary time propagation $P_n|\Psi_T\rangle$ will be suppressed by a factor $e^{-n\Delta E\Theta}$ in comparison to $P_0|\Psi_T\rangle$. In two limiting cases, we estimate $\Delta E \sim U_f/4$ for $J/t \ll 1$ and $\Delta E \sim 3U_f/8$ for $J/t, J/U_f \gg 1$. To confirm that we are well into the P_0 subspace we plot in Fig. 1 the single particle occupation number $n^{f}_{\vec{k}} \equiv \langle\Psi_0| \sum_{\sigma} f^{\dagger}_{\vec{k},\sigma} f_{\vec{k},\sigma} |\Psi_0\rangle$ with $f_{\vec{k},\sigma} = (1/L)\sum_{\vec{j}} e^{i\vec{k}\cdot\vec{j}} f_{\vec{j},\sigma}$. Our results are indistinguishable from $n^{f}_{\vec{k}} \equiv 1$ which leads to $\langle\Psi_0| \sum_{\sigma} f^{\dagger}_{\vec{i},\sigma} f_{\vec{j},\sigma} |\Psi_0\rangle = \delta_{\vec{i},\vec{j}}$, a property which may be realized only if $P_0|\Psi_0\rangle = |\Psi_0\rangle$. Owing to Eq. (5), $|\Psi_0\rangle$ is nothing but the ground state of the KLM.

We now discuss the half-filled case as a function of J/t and start with the spin degrees of freedom. To establish long-range magnetic order, we compute the quantities $S^{\alpha}(\vec{r}) = \frac{4}{3}\langle \vec{S}^{\alpha}(\vec{r}) \cdot \vec{S}^{\alpha}(\vec{0})\rangle$ as well as its Fourier transform: $S^{\alpha}(\vec{q}) = \sum_{\vec{r}} e^{i\vec{q}\cdot\vec{r}} S^{\alpha}(\vec{r})$. We consider separately the conduction ($\alpha = c$) and localized ($\alpha = f$) electrons. Long-range antiferromagnetic order is present when $\lim_{L\to\infty} S^{\alpha}(L/2, L/2) \equiv \lim_{L\to\infty} S^{\alpha}[\vec{Q} \equiv (\pi,\pi)]/L^2$ takes a finite value. Figure 2 plots both of the above quantities versus $1/L$ for the f electrons. For lattice sizes ranging from $L = 6$ to $L = 12$ the QMC data extrapolates linearly to a finite value for $J/t \leq 1.45$.

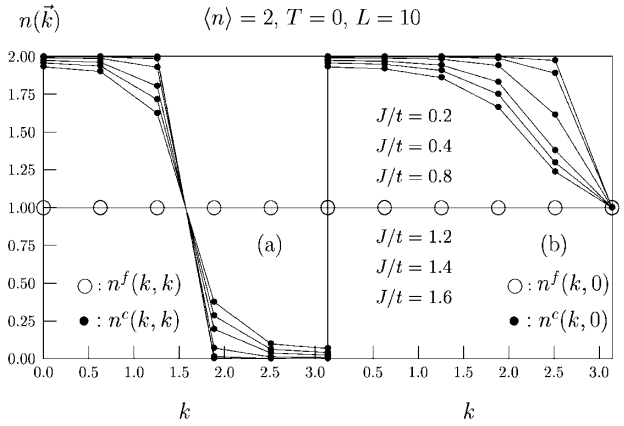

FIG. 1. Momentum distribution for the f and c electrons. (a) $\vec{k} = k(1,1)$ and (b) $\vec{k} = k(1,0)$. Within our precision, $n^{f}(\vec{k}) \equiv 1$ for all considered values of J/t. To achieve this we have chosen values U_f/t ranging from $U_f/t = 0.5$ ($J/t = 0.2$) to $U_f/t = 2$ ($J/t = 1.6$). As J/t grows, $n^{c}(\vec{k})$ becomes smoother.

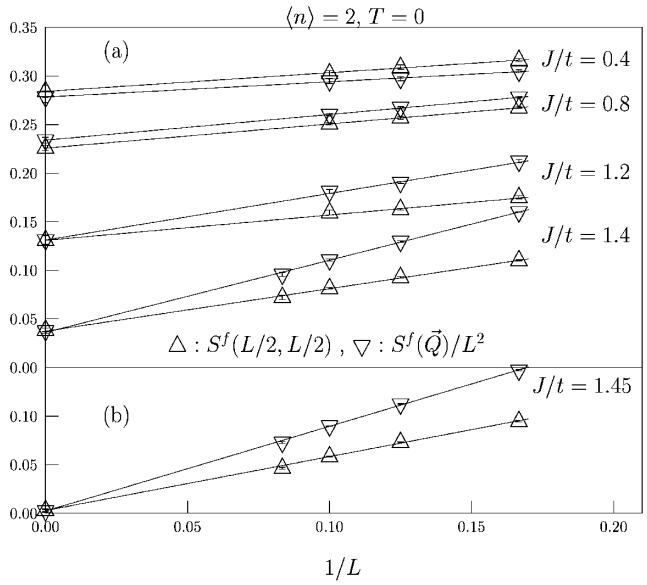

FIG. 2. Spin-spin correlations for the f electrons versus inverse linear length L for several values of J/t. The solid lines are least square fits to the form $a + b/L$. The symbol at $1/L = 0$ corresponds to the extrapolated value. As apparent, both $S^f(L/2, L/2)$ and $S^f(\vec{Q})/L^2$ scale to the same value. The staggered moment $m^{f}_{s} = \sqrt{\lim_{L\to\infty} S^f(L/2, L/2)}$.

Similar results are plotted in Fig. 3 for the conduction electrons. The resulting staggered moment $m_s^\alpha \equiv \sqrt{\lim_{L\to\infty} S^\alpha(\vec{Q})/L^2}$ is plotted versus J/t in Fig. 6 below. At $J/t = 0.2$, $m_s^f = 0.557(3)$—a value much larger than for the Heisenberg model: $m_s^H = 0.3551(3)$ [24]. In contrast, m_s^c is small at small values of J/t—$m_s^c = 0.072(6)$ at $J/t = 0.4$. In comparison, the half-filled Hubbard model at $U/t = 4$ leads to $m_s \sim 0.2$ [7]. At the mean-field level, the behavior of $m_s^{f,c}$ at weak coupling may be captured by the ansatz $\langle \vec{S}_{\vec{i}}^{\,f} \rangle = (-1)^{\vec{i}} \tilde{m}_s^f \vec{e}_z/2$ ($\tilde{m}_s^f \leq 1$) which leads to $\tilde{H}_{\mathrm{KLM}} = -t \sum_{\langle \vec{i},\vec{j}\rangle,\sigma} c^\dagger_{\vec{i},\sigma} c_{\vec{j},\sigma} + (J\tilde{m}_s^f/2) \sum_{\vec{i}} (-1)^{\vec{i}} S^c_{\vec{i}} \cdot \vec{e}_z$. Minimizing the free energy with respect to $\tilde{m}_s^f$ yields $\tilde{m}_s^f = 1$. The conduction electrons are thus subject to a staggered field of magnitude $\propto J$. Since $\mathrm{Re}\chi(\vec{Q}, \omega = 0)$ is singular, this immediately leads to long-range magnetic order with $\tilde{m}_s^c \propto (J/t)\ln^2(J/t)$ for $J/t \ll 1$. The behavior of $\tilde{m}_s^{c,f}$ bears some similarity with the QMC data (see Fig. 6 below). At larger values of J/t the Kondo effect destroys magnetic order. Both m_s^f and m_s^c scale *continuously* to zero as J/t approaches $J_c/t \sim 1.45$ (see Fig. 6 below).

Once long-range magnetic order is destroyed ($J/t > 1.45$), the ground state is expected to evolve smoothly to the strong coupling limit, $J/t \gg 1$. In this limit, $|\Psi_0\rangle$ is given by a direct product of singlets on the f-c bonds of an elementary cell. Starting from this state, a triplet excitation has a dispersion relation (up to second order in t/J) $\Delta_s^{(2)}(\vec{q}) = J - \frac{16t^2}{3J} - \frac{2t}{J}\epsilon(\vec{q})$ [11]. To compute $\Delta_s(\vec{q})$ numerically we consider $S(\vec{q},\tau) = \frac{4}{3}\langle \Psi_0 | \vec{S}(\vec{q},\tau) \cdot \vec{S}(-\vec{q},0) | \Psi_0 \rangle$ where $\vec{S}(\vec{q}) \equiv \vec{S}^f(\vec{q}) + \vec{S}^c(\vec{q})$ and $\vec{S}(\vec{q},\tau) = e^{\tau H}\vec{S}(\vec{q})e^{-\tau H}$. For $\tau t \gg 1$, $S(\vec{q},\tau) \propto \exp[-\tau\Delta_s(q)]$ with $\Delta_s(\vec{q}) \equiv E_0(S=1,N,\vec{q}) - E_0(S=0,N)$. Here $E_0(S,N,\vec{q})$ denotes the ground state energy with total spin S, momentum $\vec{q}$, and particle number $N \equiv L^2$. As in the strong coupling limit and for all considered values of J/t, the spin gap $\Delta_s \equiv \min_{\vec{q}} \Delta_s(\vec{q}) = \Delta_s(\vec{Q})$ with $\vec{Q} = (\pi,\pi)$. Figure 4a plots the raw data from which we obtain the spin gap and, in Fig. 4b, Δ_s versus $1/L$. A linear extrapolation to the thermodynamic limit leads to the results plotted in Fig. 6 below. Within our accuracy, the value of J/t for which long-range magnetic order vanishes corresponds to the value of J/t where the spin gap vanishes.

Finally, we consider the quasiparticle gap. As apparent from the single particle occupation number, $n^c(\vec{k})$ (Fig. 1), the quasiparticle gap grows continuously with growing values of J/t. To obtain an accurate estimate of this quantity, we compute $\langle \Psi_0 | \sum_\sigma c^\dagger_{\vec{k},\sigma}(\tau) c_{\vec{k},\sigma} | \Psi_0 \rangle$ which scales as $e^{-\tau\Delta_{qp}(\vec{k})}$ when $\tau t \gg 1$. Here, $\Delta_{qp}(\vec{k}) = E_0(N) - E_0(N-1,\vec{k})$. In the strong coupling limit and to first order in t/J, $\Delta_{qp}^{(1)}(\vec{k}) = 3J/4 - \epsilon(\vec{k})/2$ and thus takes a minimum at $\vec{k} = (\pi,\pi)$. Our QMC results for values of J/t ranging from $J/t = 0.4$ to $J/t = 2$ are consistent with $\Delta_{qp} \equiv \min_{\vec{k}} \Delta_{qp}(\vec{k}) = \Delta_{qp}(\pi,\pi)$ [25]. The size scaling of Δ_{qp} is presented in Fig. 5, and the extrapolated value is plotted in Fig. 6 versus J/t. As apparent, Δ_{qp} remains finite and evolves *smoothly* through the quantum transition. In the above discussed mean-field approach based on the ansatz $\langle \vec{S}_{\vec{i}}^{\,f} \rangle = (-1)^{\vec{i}} \tilde{m}_s^f \vec{e}_z/2$, the quasiparticle

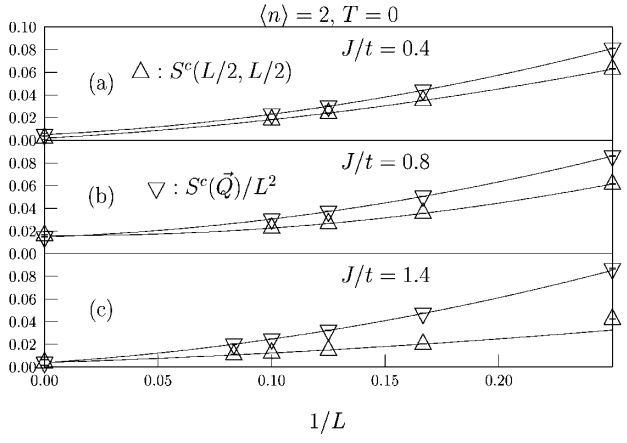

FIG. 3. Same as Fig. 2 but for the conduction electrons. In order to satisfy the relation $\lim_{L\to\infty} S^f(L/2,L/2) \equiv \lim_{L\to\infty} S^f(\vec{Q})/L^2$, we fit the data to the form $a + b/L + c/L^2$. The staggered moment $m_s^c = \sqrt{\lim_{L\to\infty} S^c(L/2,L/2)}$.

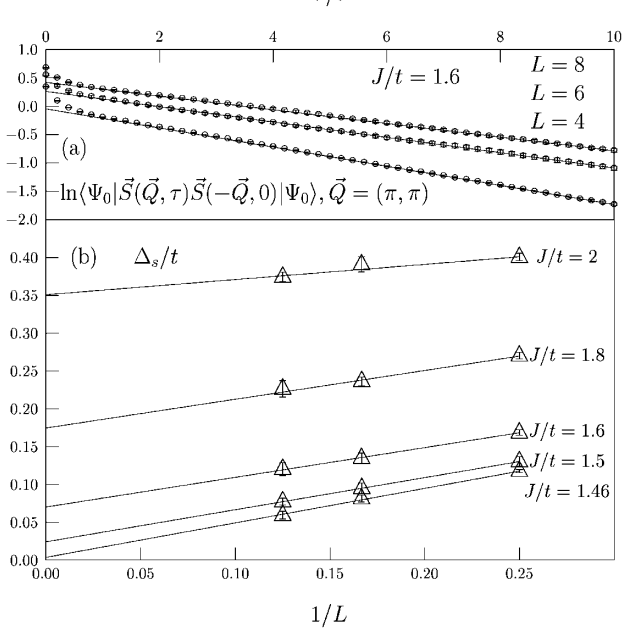

FIG. 4. (a) $\ln S(\vec{Q},\tau)$ versus τt for $J/t = 1.6$. The solid lines correspond to the least square of the tail of $S(\vec{Q},\tau)$ to the form $ae^{-\tau\Delta_s}$. The thus obtained value of the spin gap Δ_s is plotted versus $1/L$ in (b). The solid lines in (b) are least square fits to the form $a + b/L$.

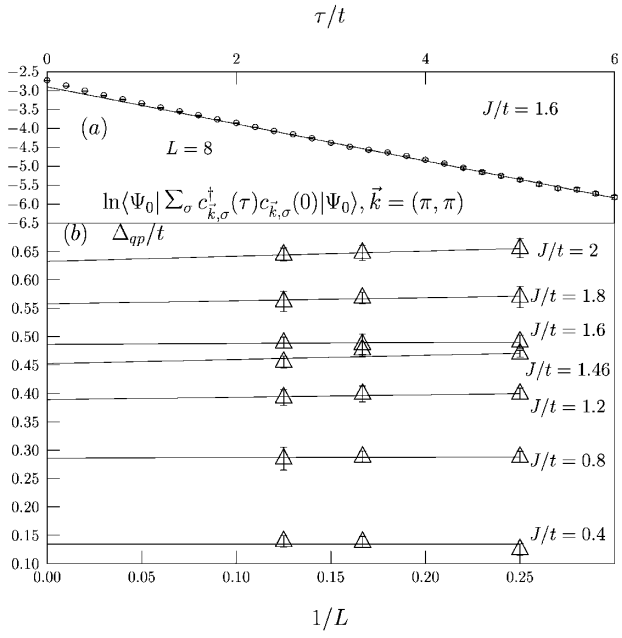

FIG. 5. Same as Fig. 4 but for the quantity $\sum_\sigma \langle \Psi_0 | c^\dagger_{\vec{k},\sigma}(\tau) c_{\vec{k},\sigma} | \Psi_0 \rangle$ so as to obtain Δ_{qp}.

gap scales as $J/4$ in the small J/t limit. Such a behavior, equally seen in one dimension [11,26], is to a first approximation consistent with our data (see Fig. 6).

In summary, we have presented an efficient auxiliary field QMC algorithm to simulate zero-temperature properties of the KLM. At half-band filling where the sign problem is absent, we calculated the staggered moment, the spin gap, and the quasiparticle gap on lattice sizes up to 12×12. Our results are summarized in Fig. 6. We observe a *continuous* quantum phase transition between long-range antiferromagnetic and spin-gapped phases. This transition occurs at $J_c/t = 1.45 \pm 0.05$ in good agreement with previous approximative results [12,13].

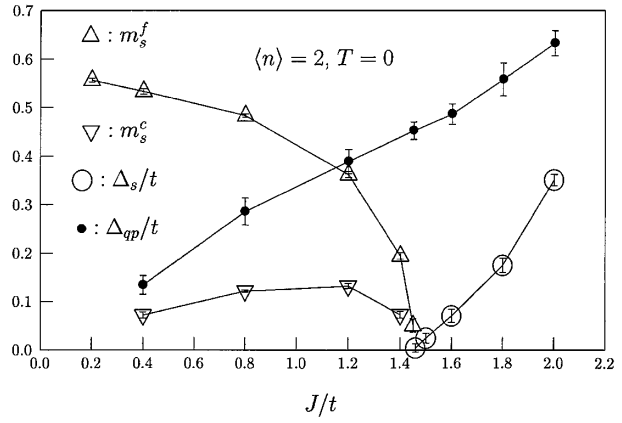

FIG. 6. Staggered moment ($m_s^{f,c}$), spin (Δ_s), and quasiparticle (Δ_{qp}) gaps of the KLM at half-band filling and $T = 0$. All plotted quantities are extrapolated to the thermodynamic limit. At $J/t = 0.2$ we were not able to distinguish m_s^c from zero.

The quasiparticle gap is finite and evolves *continuously* between both phases. Given that the charge degrees of freedom remain gapped, we expect the observed quantum phase transition to belong to the universality class of the $O(3)$ nonlinear sigma model [27,28].

A. Muramatsu is thanked for instructive conversations. The simulations were carried out on the T3E of the HLRS-Stuttgart, as well as on the T90 and T3E of the HLRZ-Jülich.

[1] P. A. Lee *et al.*, Comments Condens. Matter Phys. **12**, 99 (1986).
[2] G. Aeppli and Z. Fisk, Comments Condens. Matter Phys. **16**, 155 (1992).
[3] C. Kittel, *Quantum Theory of Solids* (Wiley, New York, 1963).
[4] K. Yosida, Phys. Rev. **147**, 223 (1966).
[5] P. W. Anderson, Phys. Rev. **124**, 41 (1961).
[6] J. R. Schrieffer and P. A. Wolff, Phys. Rev. **149**, 491 (1966).
[7] S. R. White *et al.*, Phys. Rev. B **40**, 506 (1989).
[8] M. Vekic *et al.*, Phys. Rev. Lett. **74**, 2367 (1995).
[9] C. Gröber and R. Eder, Phys. Rev. B **57**, R12 659 (1998).
[10] C. Huscroft, A. K. McMahan, and R. T. Scalettar, Phys. Rev. Lett. **82**, 2342 (1999).
[11] H. Tsunetsugu, M. Sigrist, and K. Ueda, Rev. Mod. Phys. **69**, 809 (1997).
[12] Z. Wang, X. P. Li, and D. H. Lee, Physica (Amsterdam) **199B–200B**, 463 (1994).
[13] Z. P. Shi, R. R. P. Singh, M. P. Gelfand, and Z. Wang, Phys. Rev. B **51**, 15 630 (1995).
[14] G. Sugiyama and S. Koonin, Ann. Phys. (N.Y.) **168**, 1 (1986).
[15] S. Sorella, S. Baroni, R. Car, and M. Parrinello, Europhys. Lett. **8**, 663 (1989).
[16] R. M. Fye and D. J. Scalapino, Phys. Rev. B **44**, 7486 (1991).
[17] F. F. Assaad, M. Imada, and D. J. Scalapino, Phys. Rev. B **56**, 15 001 (1997).
[18] Y. Motome and M. Imada, J. Phys. Soc. Jpn. **66**, 1872 (1997).
[19] J. E. Hirsch, Phys. Rev. B **28**, 4059 (1983).
[20] F. F. Assaad, in *High Performance Computing in Science and Engineering*, edited by E. Krause and W. Jäger (Springer, Berlin, 1998), p. 105 (cond-mat/9806307).
[21] F. F. Assaad and M. Imada, J. Phys. Soc. Jpn. **65**, 189 (1996).
[22] S. Q. Shen, Phys. Rev. B **53**, 14 252 (1996).
[23] H. Tsunetsugu, Phys. Rev. B **55**, 3042 (1997).
[24] A. W. Sandvik, Phys. Rev. B **56**, 11 678 (1997).
[25] A detailed study of the evolution of $\Delta_{qp}(\vec{k})$ as a function of J/t will be presented elsewhere.
[26] C. C. Yu and S. R. White, Phys. Rev. Lett. **71**, 3866 (1993).
[27] S. Chakravarty, B. I. Halperin, and D. R. Nelson, Phys. Rev. B **39**, 2344 (1989).
[28] A. V. Chubukov, S. Sachdev, and J. Ye, Phys. Rev. B **49**, 11 919 (1994).